

Buffer-layer-induced barrier reduction: Role of tunneling in organic light-emitting devices

S. T. Zhang, X. M. Ding, J. M. Zhao, H. Z. Shi, J. He, Z. H. Xiong, H. J. Ding, E. G. Obbard, Y. Q. Zhan, W. Huang, and X. Y. Hou^{a)}

Surface Physics Laboratory (National Key Laboratory), Institute of Advanced Materials and Technology, Fudan University, Shanghai 200433, China

(Received 1 October 2003; accepted 19 November 2003)

Based on the WKB approximation of the tunneling model, we calculate the J - V characteristics of organic light-emitting devices (OLEDs) having buffer layers of different thickness. The results show how the insertion of a buffer layer with proper thickness lowers the OLED turn-on voltage. Further calculation suggests some parameters, such as the resistivity ratio and the position of the conduction band minimum of the buffer layer relative to the lowest unoccupied molecular orbital of the organic layer, are important in selecting a buffer material. A quantitative estimation of the optimal buffer layer thickness is also presented to serve as a guide to device design. The model is validated by comparison of its predictions to experimental results. © 2004 American Institute of Physics. [DOI: 10.1063/1.1641166]

Organic light-emitting devices are currently considered as promising candidates for full-color, flat-panel displays because of their prominent advantages such as ease in fabrication and convenience in application.¹ Much effort has been made to improve the performance of the devices and to understand the physics governing their operation. It is generally recognized that enhancing the electron injection is essential for high performance devices and that proper insertion of a thin buffer layer between the electrode and the organic layer may serve this purpose. Most of the buffer materials used are insulators, including poly(methylmethacrylate) LB films,² LiF,³ Al₂O₃,⁴ SiO₂,⁵ Si₃N₄.⁶ In contrast to the conventional view that the existence of an extra insulating layer might increase the turn-on voltage, a significant decrease in turn-on voltage is usually observed in the case of the buffer-containing organic light-emitting diodes (OLEDs). The phenomenon has variously been ascribed to mechanisms such as increased tunneling probability due to reduced effective barrier,² energy level realignment induced by interfacial dipole,^{7,8} the presence of low work-function metal following the chemical reaction of buffer material,⁹ or elimination of exciton quench centers.¹⁰

Kim *et al.*² proposed that, based on Parker's model of charge tunneling through the barrier in an OLED,¹¹ the enhanced electron injection originated from a lowering of the barrier height due to a repositioning of the cathode Fermi level, E_F , with respect to the organic lowest unoccupied molecular orbital (LUMO). The energy level diagram is shown in Fig. 1. If no buffer layer is included, then upon application of a forward voltage the electron must tunnel through the barrier represented by the shaded triangle in Fig. 1(a). In the presence of a buffer layer with proper thickness, the voltage drop across the layer raises the cathode E_F by the same amount and the subsequent barrier the electrons encounter, as shown by the shaded area in Fig. 1(b), will be

smaller than in the buffer-free case, resulting in an increased injection current. Such a model can qualitatively explain the experimentally observed results but a quantitative description of the model has so far been unavailable. In this work, we present a detailed calculation based on the WKB approximation to show how the various parameters, such as the resistivity, position of the conduction band minimum (CBM) of the buffer relative to the LUMO of the organic and the thicknesses of both layers, play their roles in the model. The validity of predictions from this model is tested experimentally.

For simplicity, only the electron injection is taken into consideration and the model system used in the calculation is a single active-layer device with or without a thin buffer, as shown in Fig. 1. The current density flowing through such a device is determined by the charges incident at the cathode-organic interface multiplied by the tunneling probability¹²—if the bulk effects like space charge limitation are ignored. When a voltage V is applied, the current density $J(V)$ can be expressed as

$$J(V) = q \int \int \rho(E, p_x) f(E, p_x) T(p_x, V) dE dp_x. \quad (1)$$

Here q is the charge of an electron, ρ is the density of electronic states at the metallic cathode, E is the energy of the

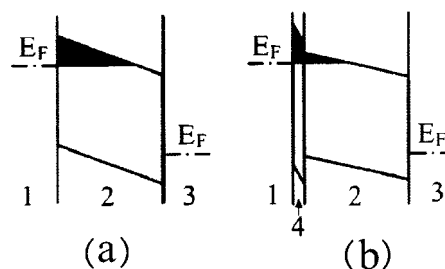


FIG. 1. Energy level diagram of devices without (a) and with (b) buffer layer after applying a voltage. 1, 2, 3, and 4 are, respectively, the cathode, the organic layer, the anode and the buffer layer inserted.

^{a)} Author to whom correspondence should be addressed; electronic mail: xyhou@fudan.edu.cn

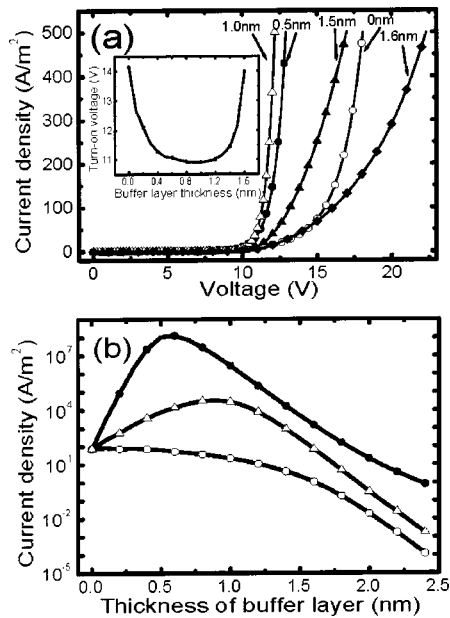


FIG. 2. (a) Calculated J - V characteristics of an OLED with buffer layers of different thickness. The open circle, the filled circle, the open triangle, the filled triangle, and the diamond represent the buffer layer thickness of 0, 0.5, 1.0, 1.5, and 1.6 nm, respectively. The inset is the turn-on voltage ($J = 50 \text{ A/m}^2$) vs the thickness of the buffer layer. The voltage reaches its minimum at a buffer layer thickness of 1.0 nm; (b) calculated dependence of current density on the thickness of buffer layer. Three curves represent different buffer-to-organic resistivity ratios: 3:1 (open circle), 5:1 (open triangle), and 10:1 (filled circle).

electron, p_x is the x component of the electron momentum, f is the Fermi-Dirac distribution function, and T is the tunneling probability. The electrons injected from the cathode are considered as free electrons. To find the tunneling probability, we use the WKB approximation

$$T(p_x, V) = \exp(-2K), \quad (2)$$

$$K = \int_{x_1}^{x_2} k(x, p_x, V) dx, \quad (3)$$

$$k(x, p_x, V) = \left[\frac{2mU(x, V) - p_x^2}{\hbar^2} \right]^{1/2}, \quad (4)$$

where $U(x)$ is the potential distribution; image force has been taken into consideration in the calculation.

It is obvious that the voltage drops across the organic and buffer layers are dependent on their resistivities and thicknesses. As a first order approximation, Ohmic law is applied to determine the ratio of the two. Considering the layer is so thin in this case that tunneling must prevail over electrons' drift in the electric field, the resistivity of the buffer film may not be the same as in its bulk form. As an example, consider Al and Alq_3 as, respectively, the metallic cathode and organic luminous material, with their E_F and LUMO -4.2 and -3.0 eV from the vacuum level. Assuming a resistivity ratio (buffer layer: Alq_3) of 5:1 and a buffer layer CBM at -1.0 eV, then the J - V characteristics for an OLED incorporating a 100 nm Alq_3 layer are calculated, including the buffer thickness as an adjustable parameter. Some of the calculated curves are shown in Fig. 2(a), with the buffer thickness equal to 0, 0.5, 1.0, 1.5, and 1.6 nm. It is clearly seen in the figure that insertion of the thin buffer

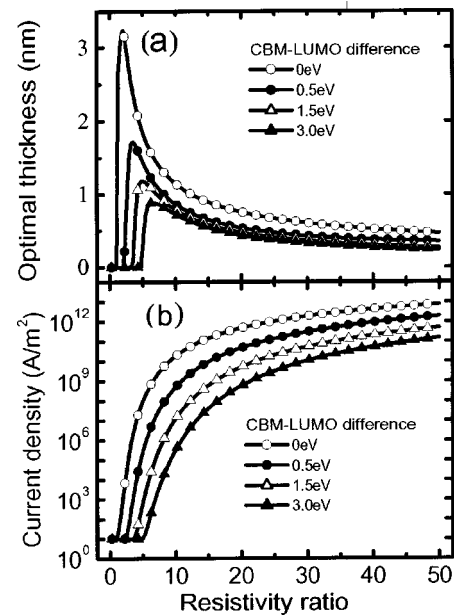


FIG. 3. (a) Relationship between optimal thickness of buffer layer and the resistivity ratio. The four curves represent various differences between the LUMO of the organic and the CBM of the buffer layer: 0 eV (open circle), 0.5 eV (filled circle), 1.5 eV (open triangle), and 3.0 eV (filled triangle); (b) Maximum possible current density vs resistivity ratio for various CBM-LUMO difference. The current density in this case means the current density achieved by inserting a buffer layer of optimal thickness.

initially displaces the characteristic J - V curve toward low turn-on voltage; for thickness greater than 1.0 nm the trend reverses. According to the present calculation, the turn-on voltage of a buffer-containing OLED, defined here as the voltage giving a current density of 50 A/m^2 , varies in a saddle-like shape with increasing buffer thickness and is minimized at the buffer thickness of about 1 nm [Fig. 2(a), inset]. This saddle-like behavior is consistent with what was previously observed.³⁻⁶

There is little doubt that the optimal buffer thickness depends on the resistivity ratio of the buffer to the organic and on the difference between the CBM level of the buffer and the LUMO level of the organic. Figure 2(b) shows the calculated dependence of the current density on the buffer thickness for selected resistivity ratios of 3:1, 5:1, and 10:1, at a fixed voltage of 15 V. The optimal buffer thickness corresponds to the highest current density available and, hence, emerges as the maximum in each curve. While the current density decreases monotonically with increasing buffer thickness and no peak appears in the case of the resistivity ratio of 3:1, one may infer from the other two cases that a higher resistivity ratio leads to a smaller optimal thickness. This is further illustrated in Fig. 3(a), where the optimal thicknesses are plotted versus the resistivity ratios, with the difference between the CBM of the buffer and the LUMO of the organic as an adjustable parameter varying from 0 to 3 eV. It is immediately evident in the figure that the optimal thickness approaches zero for low resistivity ratios because, in such cases, there is so minor a voltage drop across a buffer within the tunneling limit that the electron injection barrier can hardly be lowered by raising the E_F level of the cathode with respect to the LUMO level of the organic. The inserted buffer layer then behaves only as an extra barrier to electron

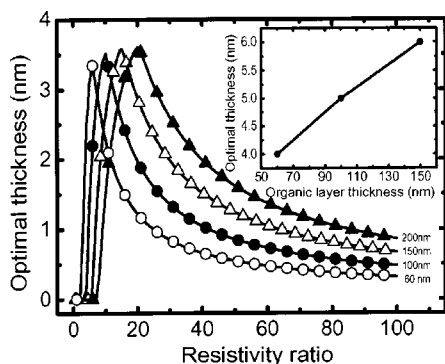


FIG. 4. Dependence of buffer layer optimal thickness on the organic layer thickness (60 nm: open circle; 100 nm: filled circle; 150 nm: open triangle; 200 nm: filled triangle). The inset shows the experimental results: the increase of the optimal thickness of sodium stearate with the thickness of the Alq_3 layer.

injection and will not improve the carrier injection efficiency. This is a possible reason why insertion of some buffer layers has been found not to decrease the OLED turn-on voltage, as reported by Kim *et al.*² Only when the resistivity ratio reaches a certain value can the E_F level be raised enough and the injection barrier accordingly lowered. Compromise between a large thickness, needed to raise the E_F level relative to the LUMO, and a small thickness, desired to minimize the extra barrier, gives rise to an optimal buffer thickness. A high-resistivity buffer will, with minimal thickness, lower the potential barrier by the same amount as a thicker buffer film of lower resistivity. The optimal thickness therefore reaches its maximum at a relatively low resistivity ratio and then drops gradually. When the CBM–LUMO difference is small, little extra potential barrier is induced and then a thicker buffer film can be inserted to raise the cathode E_F level higher. This leads to a larger optimal thickness for such cases.

Figure 3(b) shows the theoretical current density of an OLED following the insertion of a buffer layer of optimal thickness, i.e., the maximum current density that can be achieved using a given buffer material. It is seen that buffer materials with a high resistivity and a small CBM–LUMO difference will give rise to the largest current densities. Such materials are therefore most suitable to use as a buffer layer. This may serve as a guide for selecting a suitable buffer material when other factors such as interfacial effect are not taken into account.

Because the magnitude of the E_F shift is determined by the voltage drop across the buffer layer, the optimal thickness is related not only to the thickness of the buffer layer, but also to that of the organic layer. Based on the present model, the dependence of the optimal buffer layer thickness on the thickness of the organic layer is calculated and presented in Fig. 4. It is seen that, at a relatively high resistivity ratio, beyond 20, the optimal thickness increases with the organic layer thickness: at a resistivity ratio of 30, the optimal thicknesses are, respectively, 0.8, 1.4, 1.9, and 2.6 nm with the organic layer of thickness 60, 100, 150, and 200 nm. This may be understood from Fig. 1, in which maintenance of the same voltage drop across the buffer layer demands that its

thickness be increased in response to a thickening organic layer. This theoretical prediction could not be derived from other models because they involve only the interfacial effects and ignore the organic layer thickness.

Devices having structure indium tin oxide/ Alq_3 /NaSt (sodium stearate)/Al were fabricated; NaSt is chosen as buffer material for its superior thermal stability to LiF.¹³ The inset of Fig. 4 shows the increase in optimal thickness of the NaSt layer as a function of the thickness of the Alq_3 layer: the optimal thicknesses are 4, 5, and 6 nm for organic thicknesses of 60, 100, and 150 nm, respectively. This result is consistent with the preceding predictions, indicating that the simplified model adopted in the present study, in which the equivalent circuit of the buffer inserted OLED is two Ohmic resistors in series, does describe the effect of an insulating buffer on the J – V characteristics of an OLED.

By performing a numerical calculation of current density at the organic layer–cathode interface based on the WKB tunneling approximation we have succeeded in simulating the effect of inserting a buffer layer on the OLED J – V curves. The results show how insertion of an insulating buffer layer of the proper thickness lowers the turn-on voltage of the device. Further calculation suggests that a good buffer layer for electron injection should have a relatively high resistivity and a relatively low CBM level. A group of curves have been presented, which might serve as a guideline for determining the optimal thickness of a certain buffer layer. The predictions derived from this model suggest that the optimal thickness of a buffer layer is also related to the thickness of the organic layer. Although this result is not predicted by other models, experimental evidence reinforces its validity.

This work is supported by the Ministry of Science and Technology of China under the “973” project, the National Natural Science Foundation of China under Grant No. 10174013, and the Science and Technology Commission of Shanghai Municipality. The authors gratefully acknowledge much fruitful discussion with Professor X. Sun and Professor L. S. Hung.

¹C. W. Tang and S. A. VanSlyke, *Appl. Phys. Lett.* **51**, 913 (1987).

²Y. E. Kim, H. Park, and J. J. Kim, *Appl. Phys. Lett.* **69**, 599 (1996).

³L. S. Hung, C. W. Tang, and M. G. Mason, *Appl. Phys. Lett.* **70**, 152 (1997).

⁴F. Li, H. Tang, J. Andereg, and J. Shinar, *Appl. Phys. Lett.* **70**, 1233 (1997).

⁵Z. B. Deng, X. M. Ding, S. T. Lee, and W. A. Gambling, *Appl. Phys. Lett.* **74**, 2227 (1999).

⁶H. J. Jiang, Y. Zhou, B. S. Ooi, Y. W. Chen, T. Wee, Y. L. Lam, J. S. Huang, and S. Y. Liu, *Thin Solid Films* **363**, 25 (2000).

⁷S. T. Lee, X. Y. Hou, M. G. Mason, and C. W. Tang, *Appl. Phys. Lett.* **72**, 1593 (1998).

⁸T. Mori, H. Fujikawa, S. Tokito, and V. Taga, *Appl. Phys. Lett.* **73**, 2763 (1998).

⁹L. S. Hung, R. Q. Zhang, P. He, and G. Mason, *J. Phys. D* **35**, 103 (2002).

¹⁰H. Tang, F. Li, and J. Shinar, *Appl. Phys. Lett.* **71**, 2560 (1997).

¹¹I. D. Parker, *J. Appl. Phys.* **75**, 1656 (1994).

¹²A. T. Fromhold, Jr., *Quantum Mechanics for Applied Physics and Engineering* (Dover, New York, 1991).

¹³Y. Q. Zhan, Z. H. Xiong, H. Z. Shi, S. T. Zhang, Z. Xu, G. Y. Zhong, J. He, J. M. Zhao, Z. J. Wang, E. Obbard, H. J. Ding, X. J. Wang, X. M. Ding, W. Huang, and X. Y. Hou, *Appl. Phys. Lett.* **83**, 1656 (2003).